Optics and Laser Technology 130 (2020) 106373

Contents lists available at ScienceDirect

Optics and Laser Technology

journal homepage: www.elsevier.com/locate/optlastec

Full length article

Blue diode-pumped single-longitudinal-mode Pr:YLF lasers in orange spectral region

Yunshan Zhang[a], Lunbin Zhou[a], Teng Zhang[a], Yaqi Cai[a], Bin Xu[a,*], Xiaodong Xu[b], Jun Xu[c]

[a] Department of Electronic Engineering, Xiamen University, Xiamen 361005, China
[b] Jiangsu Key Laboratory of Advanced Laser Materials and Devices, School of Physics and Electronic Engineering, Jiangsu Normal University, Xuzhou 221116, China
[c] School of Physics Science and Engineering, Institute for Advanced Study, Tongji University, Shanghai 200092, China

HIGHLIGHTS

- A Pr:YLF-based single-frequency orange laser at 607 nm has been first demonstrated.
- A Pr:YLF-based single-frequency orange laser at 604 nm has been first demonstrated.
- The single-frequency orange lasers have potential application in biomedicine.

ARTICLE INFO

Keywords:
Pr:YLF crystal
Single longitudinal mode
Orange

ABSTRACT

We report on blue diode-pumped single-frequency Pr:YLF lasers in orange spectral region, for the first time to the best of our knowledge. For a single-frequency σ-polarized 607 nm laser, a maximum output power up to 175 mW is achieved with a slope efficiency of about 16.6%. Linewidth of the 607 nm single-frequency laser is measured to be about 6 MHz. Single-frequency operation has also been obtained at π-polarized 604 nm laser with a maximum output power up to 91 mW and a slope efficiency of about 8.9%. The corresponding linewidth of the 604 nm laser is about 22 MHz. The two single-frequency orange lasers exhibit wavelength tuning ranges of about 0.15 nm and 0.35 nm, respectively. This work has proposed the simplest way for single-frequency laser generation in orange spectral region, which could be obtained by complicated and low-efficiency sum-frequency mixing of Nd^{3+} lasers. This work paves a practical way for various orange-related applications.

1. Introduction

Visible single-longitudinal-mode (SLM) laser sources have a lot of important applications in precision metrology, holography and high-resolution spectroscopy [1–5]. For realizing continuous-wave visible SLM lasers, the traditional and commonly used method resorts to nonlinear frequency conversion, which have already led to SLM laser generation in red [6], green [7,8], blue [9]. Note that all these SLM lasers have been achieved via frequency doubling, which has the highest efficiency among all the nonlinear frequency conversions. In general, the extra step of nonlinear frequency conversion requires a finely temperature-controlled nonlinear crystal, which finally leads to the laser system suffering from high complexity, high cost and reduced efficiency and robustness. Moreover, orange at around 600 nm as one of the important visible wavelength region is indeed unavailable via frequency doubling of Nd^{3+} lasers because no fundamental wave at ~1.2 µm could be found from Nd^{3+}-doped materials. Sum-frequency generation is possible to generate orange lasers. For example, in 2000, Spiekermann et al. reported a 596 nm SLM orange laser with a maximum output power of 16.7 mW by sum-frequency mixing of two SLM Nd:YAG infrared lasers at 1064 nm with power of 1 W and 1357 nm with the same power [10]. This is still the only one that reported Nd^{3+}-based SLM orange laser, to our knowledge. However, the low-efficiency sum-frequency generation makes such SLM source is hard for practical application.

A more ideal route for visible laser generation, especially for SLM visible lasers, is to generate them directly, i.e. no need the extra nonlinear frequency conversion. It is well-know that trivalent praseodymium (Pr^{3+}) has suitable energy level scheme that allows Pr^{3+} lasers operating in visible spectral region [11–13]. Through the selection to longitudinal mode or the elimination of spatial hole burning effect, Pr^{3+}-doped lasers could directly realize visible SLM operation. However, to date, it has been rarely reported on the direct generation of Pr^{3+}-doped visible SLM lasers. Very recently, Luo et al. [14] reported a

* Corresponding author.
E-mail address: xubin@xmu.edu.cn (B. Xu).

https://doi.org/10.1016/j.optlastec.2020.106373
Received 9 February 2020; Received in revised form 8 April 2020; Accepted 19 May 2020
Available online 28 May 2020
0030-3992/

diode-pumped SLM Pr:YLF red laser at 640 nm with a twisted-mode cavity. It should be pointed out that red laser with high power and efficiency is still available by frequency doubling of 1.3-μm Nd^{3+} lasers or by diode lasers. However, for orange laser, especially for SLM orange laser, it seems more advisable to operate it directly from Pr^{3+} orang emission corresponding to $^3P_0 \rightarrow {}^3H_6$ transition if considering the low-efficiency sum-frequency generation and even no diode laser emitting at this spectral region. In fact, in 2008, pumping with a Ti-Sapphire laser at 821 nm, a SLM upconversion Pr,Yb:BaY_2F_8 laser at 607 nm was already obtained with a 12 mW of output power at a pump power of 2.5 W [15]. However, suffering from the low-efficiency upconversion mechanism, this result is even worse than the aforementioned one with sum-frequency generation.

With the development of biomedicine, compact SLM orange laser with high output power and efficiency are becoming more and more in demand. For example, low-noise orange laser has potential application as an excitation source for fluorescent probe in flow cytometer [16]. Pr:YLF, as the most attractive laser material for visible laser emissions, has provided quite intense emission at 607 and 604 nm orange lines with emission cross sections of about 14×10^{-20} cm^2 and 10×10^{-20} cm^2 [17,18]. In this work, we report the first demonstration of diode-pumped Pr:YLF SLM orange lasers at σ-polarized 607 nm and π-polarized 604 nm.

2. Experimental details

Experimental setup of the SLM Pr:YLF orange lasers is shown schematically in Fig. 1. An InGaN diode laser emitting at 444 nm is used as the pump source. The pump beam was focused by a 50-mm (focal length) focusing lens into the laser crystal. The resonator has a simple two-mirror plane-concave configuration. The input mirror (IM) is a flat mirror with high-transmission coating of about 92% at pump wavelength. Moreover, the IM has a high reflection of about 99.9% at the considered orange laser wavelengths and more than 78% of transmission at 640 nm to suppress this high-gain emission. The output coupler (OC) is a concave mirror with a radius of curvature of 100 mm and coated with a partial transmission of about 3.5% at the considered orange laser wavelengths. The physical length of the laser cavity was finally optimized to about 98 mm for laser operation.

The laser gain medium is an uncoated *a*-cut Pr:YLF crystal with dimensions of $3 \times 3 \times 6$ mm^3. Dopant concentrations of this Pr:YLF crystal is 0.5 at.%. Pump absorption ratio of this crystal is about 65%. Moreover, to protect this crystal from thermal fracture, we wrapped it with indium foil and then mounted it inside a water-cooled copper block with temperature set at 16 °C. Additionally, to operate SLM laser, we used two BK7 glass thin plates as Fabry-Pérot (F-P) etalons with thicknesses of 1 mm and 0.15 mm.

3. Results and discussion

When the Pr:YLF laser was operated in free-running mode, we have achieved a continuous-wave orange laser at 607 nm with a maximum output power of 376 mW at an absorbed power of 1460 mW and the laser threshold is about 140 mW, as shown in Fig. 2. The optical-to-optical efficiency is about 25.7% at maximum and slope efficiency of the laser is 28.3%. Note that the slope efficiency is very close to the previously reported results with slope efficiencies of 30.6% [15] and

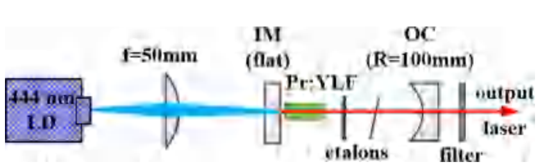

Fig. 1. Laser experimental setup of diode-pumped orthogonally polarized SLM Pr:YLF laser at 604 nm and 607 nm.

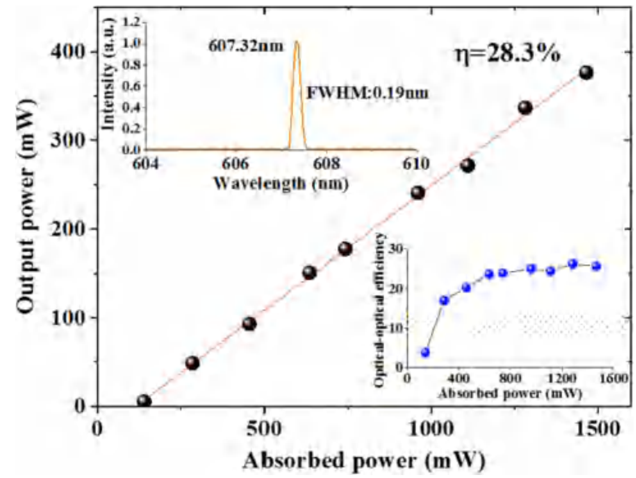

Fig. 2. Output power versus absorbed power for free-run 607 nm laser; inset: laser spectrum and the whole optical-optical efficiency.

32% [12]. We noticed that in all these works 0.5 at.% doped Pr:YLF crystal were used. However, with a 0.2 at.% doped Pr:YLF crystal, we have ever obtained a slope efficiency of 42% [16]. Hence, we ascribe the relatively low efficiency to relatively high dopant concentration of the used Pr:YLF crystal. High dopant concentration increases the probability of nonradiative cross-relaxation processes. Moreover, as we know, Pr:YLF crystal has reabsorption effect at orange, which results in high reabsorption loss if the dopant concentration is high. Furthermore, we estimate the intracavity round-trip loss L by using the following expression

$$\eta_s = \frac{\lambda_p}{\lambda_o}\eta_p\eta_e\frac{T}{T+L} \tag{1}$$

where η_s is the slope efficiency; λ_p and λ_o are the pumping wavelength and laser wavelength, respectively; η_p is the excitation quantum efficiency, i.e. the fraction of excited ions per absorbed pump photons, which can be assumed to be equal to unity; T is the transmission of output couplers; L is the intracavity round-trip loss and η_e is the average mode overlap between the pump beam and the cavity laser beam in the laser crystal, which can be estimated to be about 82% by using the same calculating steps as shown in Ref. [19]. Substituting the relevant parameters values into this expression, we can readily calculate the intracavity round-trip loss to be about 3.9%, which indicates a moderate loss for the present laser. In this work, all results were achieved under the present experimental condition with available optical components. We have not made effort on power scaling, which will be our next investigation.

The laser output light spectrum is shown as an inset in Fig. 2. The peak wavelength is at 607.32 nm and its FWHM is about 0.19 nm, measured with an optical spectrum analyzer with resolution of 0.08 nm. The longitudinal mode spacing can be simply calculated to be about 0.00183 nm (1.48 GHz). Thus, the present 607 nm orange laser contains about 104 longitudinal modes. We measured the stability of the maximum output power to be about 3.1% in 20 min, which indicated there existing a moderate multimode competition.

A common way to achieve SLM laser is to insert, within the cavity, one or more etalons [20–22]. In this experiment, we have considered the realization of compact and cost-effective SLM laser operation by inserting two etalons with thicknesses of 1 mm and 0.15 mm. The thick etalon is required to discriminate against adjacent longitudinal modes of the cavity. The thin etalon must then discriminate against the adjacent transmission maxima of the thick etalon. Note that, at the same time, usage of the etalons is of advantage for wavelength tuning. Transmission of an etalon can be written as

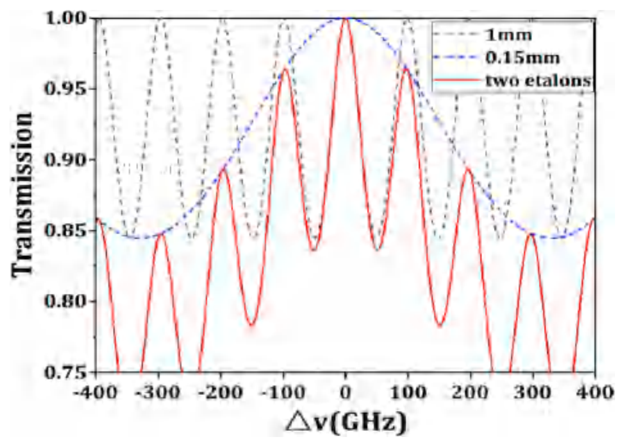

Fig. 3. The individual transmissions of F-P etalons with thicknesses of 1 mm and 0.15 mm (dashed curve) and combined transmission of two etalons (solid curve).

$$T = \frac{(1-R)^2}{(1-R)^2 + 4R\mathbf{sin}^2\left(\frac{2\pi n l_e \mathbf{cos}\theta}{\lambda}\right)} \tag{2}$$

where R is the reflectivity for one surface of etalon, n and l_e the refractive index and thickness of etalon, λ the wavelength, and θ the refraction angle inside the etalon. It is clear that the tilt angle is a crucial factor that affects the transmission of some a potential laser emission. We further plots the specific transmission curves of our case in Fig. 3. The two dashed lines show the individual transmissions of the two etalons and the solid line stands for the final transmission after the two etalons, i.e. combined transmission. From this figure, one can see that the maximum transmissions of the etalon group is determined by the thinner etalon. However, the etalon group has a far larger transmission difference, similar to the thicker etalon, than the thinner etalon. As a result, the etalon group has enhanced capacity in wavelength discrimination. We can adjust the angle of the etalons and make sure only one mode is in the peak of the transmission and has the highest gain whereas the other modes suffer high losses and are suppressed.

During the experiment, we first inserted the 0.15-mm etalon into the laser cavity. Under this situation, the maximum output power reduced to 293 mW. Then, using a scanning F-P interferometer (SA200-5B, Thorlabs) with a FSR of 1.5 GHz and resolution of 7.5 MHz, we observed the longitudinal mode at maximum output power, as shown in Fig. 4, from which one can see that the laser is very close to SLM

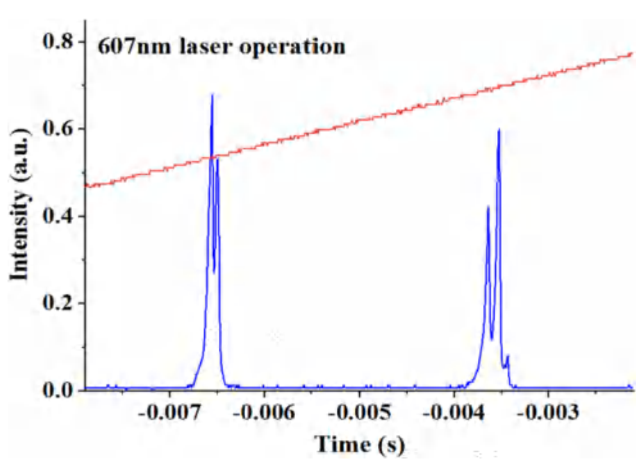

Fig. 4. A F-P interferometer scanning spectra of 607 nm laser with much reduced longitudinal mode numbers under the introduction of the 0.15-mm etalon.

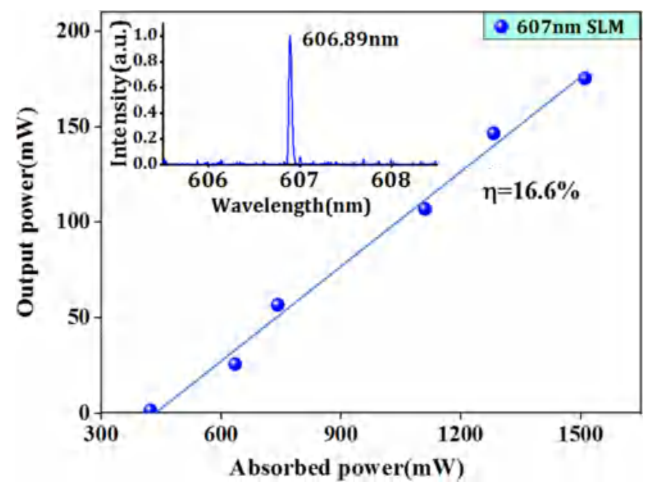

Fig. 5. Output power versus absorbed power of the SLM laser at 607 nm; Insets: the corresponding laser spectrum.

operation. To ensure a real SLM operation, we then inserted the 1-mm etalon vertically into the laser resonator. By further finely tuning the 0.15-mm etalon, we have firstly operated the SLM operation at 607 nm and the laser performance is shown in Fig. 5. The maximum output power is 175 mW with a slope efficiency of 16.6%. The corresponding laser spectrum shows a peak at 606.89 nm with FWHM of about 0.036 nm. The peak wavelength shift should be explained by the wavelength-dependent transmission of the etalons. Compared with multimode operation, the single-frequency laser performance (output power and efficiency) is mainly degraded owing to additional losses of the etalons. The FWHM measurement may be limited by the resolution of the optical spectrum analyzer (OSA).

The longitudinal mode of the Pr:YLF laser was monitored by the scanning F-P interferometer. Fig. 6 shows the measuring results of the interferometer at maximum output powers of the 607 nm laser. The stable scanning spectrum with adjacent frequency spacing of 1.5 GHz indicate the lasers operating in SLM state. The details, as shown in Fig. 6 (b), show the linewidth of the 607 nm laser to be about 6 MHz corresponding to about 7.3×10^{6} nm, which is far smaller than 0.036 nm as the above measured value with the OSA. Therefore, this result clearly indicates that resolution of the OSA is not enough as we

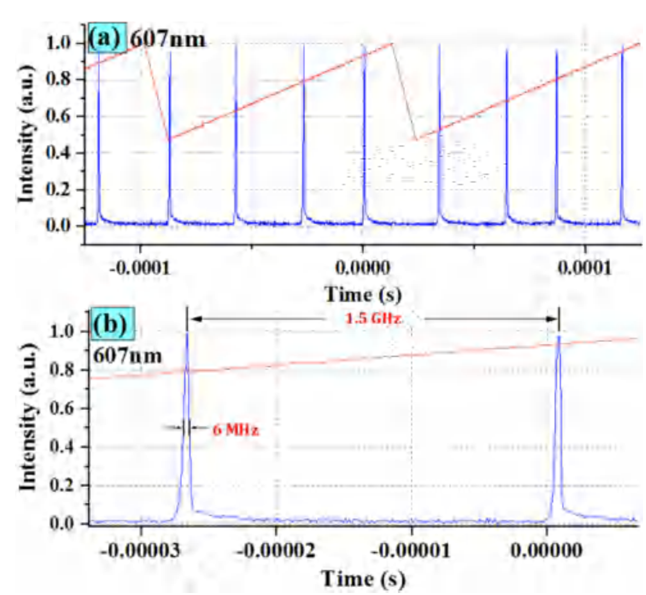

Fig. 6. (a) F-P interferometer scanning spectrum and (b) linewidth measurement of the 607 nm SLM laser.

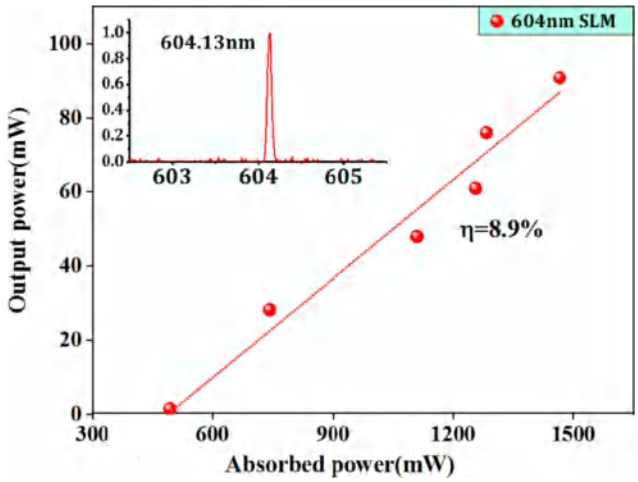

Fig. 7. Output power versus absorbed power of the SLM laser at 604 nm; Insets: the corresponding laser spectrum.

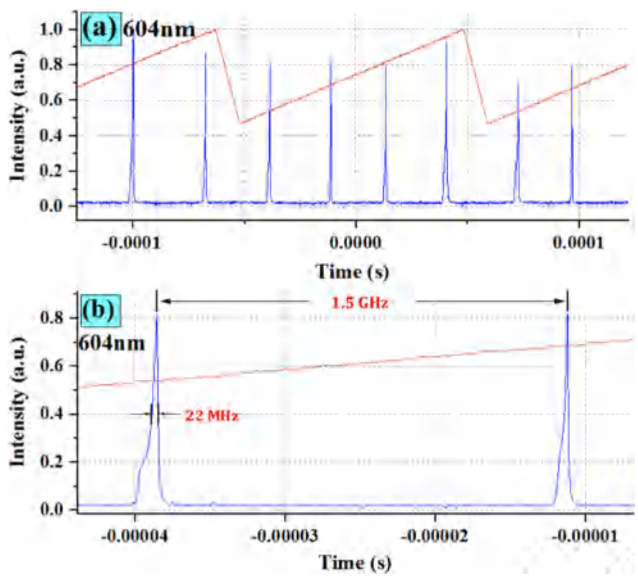

Fig. 8. (a) F-P interferometer scanning spectrum and (b) linewidth measurement of the 604 nm SLM laser.

mentioned above. In fact, the linewidth measurement could also be limited by resolution of the F-P interferometer. So, real linewidth of the achieved 607 nm laser might narrower than 7.3×10^{-6} nm.

By tilting the 0.15-mm etalon slightly, we found that the lasing wavelength of the 607 nm laser can shift to 604 nm. For the SLM 604 nm laser, the achieved maximum output power is 91 mW and the slope efficiency is linearly fitted to be about 8.9% (see Fig. 7). The laser spectrum peaks at 604.13 nm. Fig. 8 shows the scanning result of the 604 nm laser with a linewidth of about 22 MHz corresponding to about 2.7×10^{-5} nm. The wavelength shift from 607 nm to 604 nm should be explained by the introduction of the etalon group, which led to suitable intracavity loss difference for the two emission lines. In fact, according to our calculation, just by tilting the 0.15-mm etalon to an angle of about 4.5° (angle θ), the etalon group provides a transmission of 100% for 604 nm line while a transmission of about 76.8% for 607 nm line, i.e. a transmission difference of about 23.2%.

One may notice that the power data shown in Fig. 7 and even in Fig. 5 are not so linear compared with that achieved from free-run laser operation as shown in Fig. 2, which should be explained by the insertion of the etalon. To ensure stable operation of the two single-frequency lasers from thresholds to maximum output powers, we must carefully re-orientate the etalon at each output power, which led to the whole power data deviating from linearity. However, for the two single-frequency laser operation (607 nm and 604 nm), their maximum output powers are quite stable with power stabilities of about 0.5% (607 nm SLM) and 0.7% (604 nm SLM). Moreover, no obvious mode hopping can be found for all the SLM lasers by observing the resolution-limited optical spectrum analyzer.

Last but not least, it is worthwhile to report that the two SLM orange lasers both exhibit a certain wavelength tunings by slightly titling the 0.15-mm etalon. The tuning ranges are respectively to be about 0.15 nm for the 607 nm SLM laser and 0.36 nm for the 604 nm SLM laser.

4. Conclusion

In conclusion, we have demonstrated diode-pumped SLM Pr:YLF lasers at 607 nm and 604 nm. The two single-wavelength SLM lasers at 607 nm and 604 nm were achieved with maximum output powers of 175 mW and 91 mW. Their linewidths were also measured to be about 6 MHz and 22 MHz, respectively. Wavelength tunings of the two SLM lasers were obtained with ranges of 0.15 nm for the 607 nm emission and 0.35 nm for the 604 nm emission. Power scaling of the present orange SLM lasers could be confidently realized by optimizing optical quality of the laser crystal, dopant concentration and length of the laser crystal. This work presents a simple way for realizing orange SLM laser for potential applications.

CRediT authorship contribution statement

Yunshan Zhang: Investigation, Data curation, Writing - original draft. **Lunbin Zhou:** Investigation, Formal analysis. **Teng Zhang:** Visualization. **Yaqi Cai:** Software. **Bin Xu:** Conceptualization, Methodology, Project administration, Supervision, Writing - review & editing. **Xiaodong Xu:** Resources. **Jun Xu:** Resources.

Declaration of Competing Interest

The authors declare that they have no known competing financial interests or personal relationships that could have appeared to influence the work reported in this paper.

References

[1] A.N. Vlasov, Single-frequency He-Ne laser for linear measurements, Proc. SPIE 3345 (1997) 37–39.
[2] T.F. Jin, R.F. Batch, R. Kecke, Diode pumped single frequency coupled cavity $Nd:YVO_4$ laser at 532 nm wavelength, SPIE 3613 (1999) 16–22.
[3] M.V. Okhapkin, M.N. Skvortsov, A.M. Belkin, N.L. Kvashnin, S.N. Bagayev, Tunable single-frequency diode-pumped Nd:YAG ring laser for 1064/532 nm for optical frequency standard applications, Opt. Commun. 203 (3) (2002) 359–362.
[4] M. Jacquemet, F. Druon, F. Balembois, P. Georges, Blue-green single-frequency laser based on intracavity frequency doubling of a diode-pumped ytterbium-doped laser, Opt. Express 13 (7) (2005) 2345–2350.
[5] H.F. Zhang, M.L. Long, H.R. Deng, Z.B. Wu, Z.E. Cheng, Z.P. Zhang, Space debris laser ranging with a 60 W single-frequency slab nanosecond green laser at 200 Hz, Chin. Opt. Lett. 17 (5) (2019) 051404.
[6] R. Sarrouf, V. Sousa, T. Badr, G. Xu, J.J. Zondy, Watt-level single-frequency tunable Nd:YLF/periodically poled $KTiOPO_4$ red laser, Opt. Lett. 32 (18) (2007) 2732–2734.
[7] G.K. Samanta, S.C. Kumar, M.E. Zadeh, Stable, 9.6 W, continuous-wave, single-frequency, fiber-based green source at 532 nm, Opt. Lett. 34 (10) (2009) 1561–1563.
[8] W. Wang, H.D. Lu, J. Su, K.C. Peng, Broadband tunable single-frequency $Nd:YVO_4$/LBO green laser with high output power, Appl. Opt. 52 (11) (2013) 2279–2283.
[9] F.Q. Li, B. Zhao, J. Wei, P.X. Jin, H.D. Lu, K.C. Peng, Continuously tunable single-frequency 455 nm blue laser for high-state excitation transition of cesium, Opt. Lett. 44 (15) (2019) 3785–3787.
[10] S. Spiekermann, H. Karlsson, F. Laurell, I. Freitag, Tunable single-frequency radiation in orange spectral region, Electron. Lett. 36 (2000) 543–545.
[11] A. Richter, E. Heumann, E. Osiac, G. Huber, W. Seelert, A. Diening, Diode pumping of a continuous-wave Pr^{3+}-doped $LiYF_4$ laser, Opt. Lett. 29 (22) (2004) 2638–2640.
[12] B. Xu, P. Camy, J.L. Doualan, Z. Cai, R. Moncorgé, Visible laser operation of Pr^{3+}-

doped fluoride crystals pumped by a 469 nm blue laser, Opt. Express 19 (2) (2011) 1191–1197.
[13] T. Gün, P. Metz, G. Huber, Power scaling of laser diode pumped Pr^{3+}:$LiYF_4$ cw lasers: efficient laser operation at 522.6 nm, 545.9 nm, 607.2 nm, and 639.5nm, Opt. Lett. 36 (6) (2011) 1002–1004.
[14] S. Luo, Z. Cai, H. Xu, Z. Shen, H. Chen, L. Li, Y. Cao, Direct oscillation at 640-nm in single longitudinal mode with a diode-pumped Pr:YLF solid-state laser, Opt. Laser Technol. 116 (2019) 112–116.
[15] T.H. My, Ph. Goldner, O.G. Noel, M. Tonelli, F. Bretenaker, Single-frequency operation of an orange avalanche upconversion laser for high-resolution laser spectroscopy, Eur. Phys. J. Appl. Phys. 42 (2008) 121–124.
[16] V. Kapoor, V. Karpov, C. Linton, F.V. Subach, V.V. Verkhusha, W.G. Telford, Solid state yellow and orange lasers for flow cytometry, Cytom. Part A 73A (2008) 570–577.
[17] Q. Tian, B. Xu, N. Li, Z. Luo, H. Xu, Z. Cai, Direct generation of orthogonally polarized dual-wavelength continuous-wave and passively Q-switched vortex beam in diode-pumped Pr:YLF lasers, Opt. Lett. 44 (22) (2019) 5586–5589.
[18] B. Xu, Z. Liu, H. Xu, Z. Cai, C. Zeng, S. Huang, Y. Yan, F. Wang, P. Camy, J.L. Doualan, A. Braud, R. Moncorge, Highly efficient InGaN-LD-pumped bulk Pr:YLF orange laser at 607 nm, Opt. Commun. 305 (2013) 96–99.
[19] J. Lan, Y. Wang, X. Huang, Z. Lin, B. Xu, H. Xu, Z. Cai, X. Xu, J. Xu, Single- and dual-wavelength lasers of diode-pumped Nd:LuYAG mixed crystal on various $^{4}F_{3/2} \rightarrow$ $4_{I13/}2$ Stark-level transitions, J. Phys. D Appl. Phys. 49 (2016) 305101.
[20] L. Wang, C.Q. Gao, M.W. Gao, L. Liu, F.Y. Yue, Diode-pumped 2 μm tunable single-frequency Tm:LuAG laser with intracavity etalons, Appl. Opt. 52 (6) (2013) 1272–1275.
[21] T.Y. Dai, Y.L. Ju, B.Q. Yao, Y.J. Shen, W. Wang, Y.Z. Wang, Single-frequency, Q-switched Ho:YAG laser at room temperature injection-seeded by two F-P etalons-restricted Tm, Ho:YAG laser, Opt. Lett. 37 (11) (2012) 1850–1852.
[22] X.L. Zhang, L. Li, J.H. Cui, Y.L. Ju, Y.Z. Wang, Single longitudinal mode and continuously tunable frequency Tm,Ho:YLF laser with two solid etalons, Laser Phys. Lett. 7 (3) (2010) 194–197.